June 2002 Technical Report: KUL/ESAT/PSI/0202

# Computer Aided Detection of Colonic Polyps via Geometric Features Classification

G. Kiss, J. Van Cleynenbreugel,
M. Thomeer, P. Suetens
and G. Marchal

Katholieke Universiteit Leuven - Center for Processing Speech and Images

PSI

Kasteelpark Arenberg 10
B-3001 Heverlee, Belgium

Telephone: +32-(0)16-32.17.13 Fax: +32-(0)16-32.17.23
http://www.esat.kuleuven.ac.be/psi

LEUVEN

# Computer Aided Detection of Colonic Polyps via Geometric Features Classification

Gabriel Kiss, Johan Van Cleynenbreugel, Maarten Thomeer,
Paul Suetens and Guy Marchal

Faculties of Medicine & Engineering,
Medical Image Computing (Radiology - ESAT/PSI),
University Hospital Gasthuisberg
Herestraat 49, B-3000, Leuven, Belgium
Email: Gabriel.Kiss@uz.kuleuven.ac.be

## Abstract

We present a system for Computer Aided Diagnosis in Virtual Colonography based on geometric model fitting. Our approach extends surface normal analysis and sphere fitting methods. We label locations in the volume data, which have a high probability of being colonic polyps, and present them in a user-friendly way. The method was tested on a study group of 52 data sets. Using normal colonoscopy as standard of reference, true positive and false positive findings were determined. The detection rate for polyps larger than 6mm was above 90%. We introduce a classification scheme based on neural networks to be able to reduce the number of false positive cases. Initial results show that Computer Aided Diagnosis is feasible and that our method holds potential for screening purposes.

## 1 Introduction

Colorectal neoplasms can be defined as a spontaneous growth of tissue forming an abnormal mass. The colorectal neoplasm is the precursor of colorectal cancer, one of the most common types of cancer and the second leading cause of cancer-related deaths in the industrialized world [1]. Fortunately early detection and treatment of colonic neoplasms can prevent colonic cancer. For patients who receive early treatment the survival rate after five years is 92%, when adjacent organs or lymph nodes are affected it drops to 64% and when distal organs are reached only 7% of patients are alive after five years [2]. These figures show that early detection of neoplasms is an effective way of reducing the incidence of colonic cancer.

Many detection methods are available, these include occult blood testing, barium enema examinations, sigmoidoscopy, colonoscopy, virtual colonography and lately genetic testing. From all these methods colonoscopy has the highest accuracy and it is widely considered as a gold standard but it is invasive and costly, properties not suitable for a screening method. So far only occult blood testing (testing for blood in the stool) was used as a screening method but it suffers from a low sensitivity and specificity.

Virtual colonography was introduced in 1994 by Vining et. al. [3] and is a method for exploring the colonic area hinging on volumetric image data (data acquired using CT or MR). CT Colonography (CTC) uses CT data to evaluate the colonic wall and it is still the method of preference despite of the ionizing radiation. The reason for this lies in the fact that patient preparation for CTC is less invasive as for MR Colonography. CTC can be still considered a new method due to ongoing technical innovations (spiral, multi-slice CT). As a matter of fact there is no consensus on issues like patient preparation, scanning protocols and data analysis [4].

Early data analysis has concentrated only on data visualization. The goal was to find the "best" visualization technique, which offers the most of clinical information in the shortest time. The visualization component for CTC covers now a range of components ranging from well established techniques like 2D axial slices and 3D multi-planar and reformatted images towards more experimental ones like virtual double contrast imaging, sliding thin slabs, virtual colonoscopy, 3D unfolded cube, flattened/unfolded colon.

However CTC suffers from perceptual errors, the accuracy depends on the visualization method and there is a learning curve involved. Moreover the expected increase in image volume size (soon 1024 voxels in each dimension), makes it clear that automated methods are needed for polyp detection. Computer Aided Diagnosis (CAD) is one possible approach to improve reading efficiency and accuracy and consists in automatic detection of conspicuous masses that resemble polyps. Due to rather low specificity of CAD, its results are presented to the reading radiologist who makes the final diagnosis.

## 2 Method

The purpose of this paper is to present a possible CAD approach for CTC. This method is based on our previous developments [5] and as opposed to the previous one concentrates on finding not only polyps larger than 10mm, but smaller polyps as well. Most of the CAD algorithms contain two steps a generation step (polyp candidates are generated) and a testing step (final polyp candidates are selected based on the previously determined set). In fact the testing step tries to detect and eliminate the false positive findings generated by the first step.

Our previous method finds polyp candidates based on their geometric features, followed by a non-maximum suppression algorithm to extract the final candidates. While this approach gives acceptable results for large polyps it fails for smaller ones. Thus the need for a more elaborated testing (classification) step was obvious. Also the generation step was improved to include smaller polyps in the initial candidates set.

In fact, colonic neoplasms can be classified into protruded (polypoid) type and superficial (non-polypoid) type. The polypoid types resemble structures of spherical (with stalk) or semi-spherical (without stalk) appearance. The polypoid types have a height of at least 3mm. The superficial neoplasms have a height smaller than 3mm and can be classified into flat adenomas, laterally spreading carcinomas and depressed type carcinomas. With the current method we want to detect all the protruded type polyps and from the superficial polyps we can theoretically detect only flat adenomas (which can be seen as small (5 mm) polyps). The response on the laterally spreading neoplasms resembles the response obtained on haustral folds, while the depressed type is essentially concave and it will be missed by the generation step already.

The novelty of the method is the computation of features, which are based entirely on implicit properties resulting from the generation step. Using this technique there is no need for explicit segmentation of polyp candidates, a difficult task is some cases. As compared to the previous approach the classification step was elaborated, consisting now in a feature based classification using a probabilistic network. One of the disadvantages of the previous method was the large number of threshold parameters. This was improved either by automatically determining threshold values or by fixing the values of some parameters.

The next subsections will present the method as follows: first the previous method (which can be considered as a generation technique) is described, followed by a presentation of the extraction of implicit features. Finally the classification step is detailed.

### 2.1 Generation

The generation step has the following steps: segmentation, normal incidence analysis and 3D Hough transform based sphere fitting.

#### 2.1.1 Segmentation

In this step the colonic wall is determined. Since CTC images have a large contrast between (insufflated) colonic air and the colonic wall, classic region growing algorithms [8] can be used successfully. CTC preparation may influence the segmentation technique. In our case wet preparation was used and thus a substantial amount of fluid remained in the colon. Also in some patients collapsed colonic regions (due to inadequate distension) were present. Therefore multiple seed points were used to initialize the region-growing algorithm.

Previously the threshold value for the region-growing algorithm was interactively established. Now we use the method of Wiemker [9], to determine it automatically. This method computes the cumulative Laplacian histogram of the image volume and then assumes that important changes occur around its local maxima. Due to the large volumes, we are dealing with, a computation of the

cumulative Laplacian histogram on the whole volume is not feasible that is why it was computed on slices situated around the seed points. Also an initial guess $T_{guess}$ for $T_{segment}$ (based on 18 sample data sets) was computed. The final segmentation threshold $T_{segment}$ is considered to be the local maxima around $T_{guess}$. The search interval is considered as $[T_{guess} - \delta * 2, T_{guess} + \delta * 2]$, where $\delta$ is the standard deviation of the $T_{segment}$ values on the sample data sets.

Given this $T_{segment}$, for all the seed voxels a region $A$ of connected air voxels (CT value smaller than $T_{segment}$) is grown outwards in a breadth first manner. The colonic wall is defined as the set $W$ of voxels adjacent to $A$ and having an intensity value higher than $T_{segment}$. For each voxel of $A$ 6 direct neighbors are taken into consideration.

The final result of the segmentation algorithm is thus the set $W$ of disjunctive regions representing voxels on the colonic wall. It has to be mentioned that some voxels in $W$ represent in fact colonic fluid and not actual colonic wall.

### 2.1.2 Normal incidence analysis

From the voxels of $W$ only a small number will turn into actual polyp candidates. The spherical nature of the polyps suggests looking for convex surface patches. Also the colonic wall is mostly concave and will be eliminated at this step already. To estimate curvature properties one can use methods based on differential geometry, such as principal, mean and Gaussian curvatures. However we employ a simple geometrical approach to estimate the local curvature.

For each voxel belonging to $W$ we compare the normals to the colonic surface in the current point and in its neighbors. The normal to the colonic wall is computed using a Zucker-Hummel operator [8] and is perpendicular to the wall and oriented from air towards tissue. Let $p_1$ be the current point, $p_2$ a neighboring point and $g_1$, $g_2$ the image gradients in $p_1$ and $p_2$ respectively. The equation of the tangent plane to $W$ in $p_1$ is given by $p \bullet g_1 = p_1 \bullet g_1$, where $\bullet$ is the dot product. The line through $p_2$ along the direction $g_2$ has the equation $p = p_2 + r.g_2$; its intersection point $p_3$ with the tangent plane corresponds to $r = (p_1 - p_2) \bullet g_1 / g_1 \bullet g_2$. The relative position of voxels $p_2$ and $p_3$ along the direction $g_2$ is exploited to asses the convexity or concavity of the colon's surface in $p_1$, as shown in Figure 1 (left). Furthermore for a presumed convexity a $T_{convex}$ threshold is applied to the distance $l = \| p_2 - p_3 \|$.

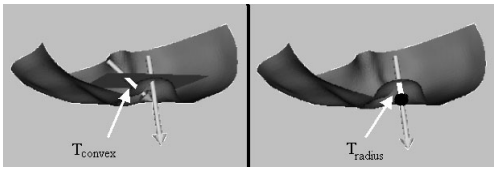


Figure 1: 3D illustration of the normal incidence analysis (left) and sphere center generation (right).

The value of $T_{convex}$ can be determined analytically as follows. Consider a perfect sphere of radius $r_p = 3.5mm$ (similar to a 7mm polyp), assume that a positive detection is wanted for an angle larger then $\theta = \pi/4$ then the value of $T_{convex}$ is:

$$\cos\theta = \frac{r_p}{r_p + T_{convex}} \Rightarrow T_{convex} = r_p * \frac{1 - \cos\theta}{\cos\theta}$$

For the given values the obtained convexity threshold is $T_{convex} = 1.45mm$.

For $p_1 \in W$, a bounding box B is defined. For each $p_2 \in B \cap W$, the described process is repeated, and the values $V_c$ and $V_t$ are computed. $V_c$ is the number of voxels situated in $B \cap W$ that satisfy $T_{convex}$, while $V_t$ is the total number of voxels in $B \cap W$. Finally those $p_1$ for which $V_c/V_t$ is higher than $T_{hits}$ are included in the set $T$ (voxels meeting the convexity threshold criteria).

By computing the value of $l$ we get for free all the voxels situated on convex surfaces too ($l > 0$), using a similar method as the one presented above. We memorize all of these voxels as well, as the set $R$ (voxels meeting the relaxed convexity criteria). Their usefulness will be shown at the end of this subsection.

Previously, the bounding box was considered as a cube around $p_1$. But, from the definition of $T_{convex}$, it is obvious that voxels close to $p_1$ will not meet the convexity criteria. Furthermore we can compute the distance from which the convexity criteria is expected to be fulfilled. This is given by:

$$d = r_p * \theta = r_p * \frac{\pi}{4} \Rightarrow d = 2.75\ mm$$

Indeed experimentally we determined that voxels closer to $p_1$ than $d$ account on average only for 0.25% from the total number of voxels. The reasons for those detections are some sharp edges we

are not interested in anyhow. Given this, the bounding box is considered as a cube with an empty core (see Figure 2). If the size of the core is set to $2*d$ the computation time required by this step is reduced to 70% of its original value.

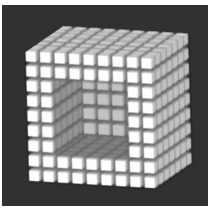

Figure 2: The considered neighborhood for the normal incidence analysis.

The last step of the normal incidence analysis is to reduce positive detections generated by noise (such as small blobs and sharp edges). To do this we extract clusters of connected voxels from the set $T$. The larger the size of the cluster, the higher the probability of being an interesting location. That is why we retain only clusters having at least $T_{cluster}$ elements. The other clusters are considered to be generated by noise and are eliminated.

Of course, polyps are not exactly spherical structures and some voxels on them will not be included in the set $T$. This is not wanted since our sphere-fitting scheme requires as much of the polyp voxels as possible, in order to generate the expected results. That is why each extracted cluster is "enhanced" (using a region growing algorithm) by including all the neighboring voxels from $R$.

#### 2.1.3 Hough transform based sphere fitting

This step is intended to exploit the spherical properties of polyps as opposed to the cylindrical properties of haustral folds. A 3D Hough transform is applied to the relaxed clusters, the goal being to generate a Hough accumulator. Given a radius $T_{radius}$ of an imaginary fitting sphere, each candidate is assumed to be on the surface of the sphere, while the local gradient in that point is perpendicular to the surface of the sphere and pointing towards its center. Figure 1 (right) presents the principle of the sphere center generation step.

The resulting Hough accumulator contains for each candidate, the number of 'voters' and the normalized image gradients (we will call normals). Because folds have a cylindrical shape the centers given by such structures will be dispersed along a line. For polyps however these centers will converge towards a small area.

The value for $T_{radius}$ needs to be selected in close correspondence with the polyps to be detected. Previously multiple passes for different $T_{radius}$ values were used. We modified this approach and construct a Hough accumulator, in which for each voxel multiple sphere centers along the local gradient are generated. By this we can handle different polyp sizes and also the irregularities of polyps which are not perfect spheres. At the moment each center has the same weight, but this could be changed allocating different weights to different polyp sizes.

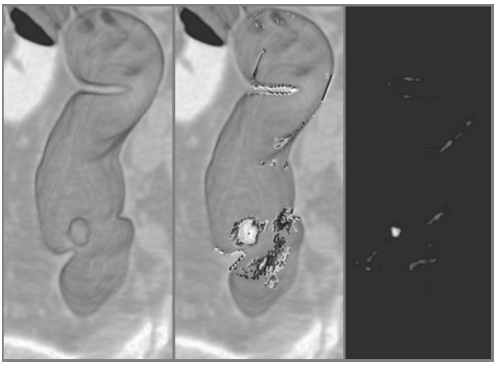

Figure 3: Figure presenting the generation step. Starting from the original CT slice (left) candidate voxels are generated (center), finally the Hough accumulator is computed (right). Candidate voxels colored in white are belonging to the set T, while the black ones are the voxels from R included during the "enhancement" step.

The results of the normal incidence analysis and sphere fitting steps are presented in Figure 3.

### 2.2 Feature extraction

Since the intention is to apply a feature classifier, we need to compute features, which will be considered as input for the classifier. Some are implicit features others will be computed based on intermediate results (like the sphere center map). Of course we need "expressive" features to characterize each of the possible classes. The normal anal-

ysis will generate positive results for the following classes: polyps, convex colonic wall, haustral folds and colonic stool or fluid.

The following features were computed: maximum value in Hough accumulator, weighted value in Hough accumulator, normal distribution, the three axis of the ellipsoid resulting after a greedy region growing algorithm, the three axis of the ellipsoid resulting after a distance weighted region growing algorithm.

We start by generating candidates based on the value in the Hough accumulator. They are generated using a non-maximum suppression algorithm. For each candidate the technique gives the maximum value in the accumulator, lets denote it $V_{max}$. To eliminate responses generated by noise we compute the weighted value ($V_{weighted}$) in the sphere centers map. This in computed as:

$$V_{weighted} = \alpha * V_{max} + (1-\alpha) * mean(V_{neighbors})$$

with $\alpha$ constant and controling the degree of smoothing.

The difference between polyps and haustral folds is made by exploiting their response to the Hough method. Polyps give converging sphere centers, while folds give dispersed centers along a curve, which follows the shape of the haustra.

The local features are evaluated by using the local normal information of each candidate. Normals generated by folds are almost coplanar while those generated by polyps have a large variance. We measure this spatial distribution by taking a reference plane defined by the center point and two randomly chosen normals. For the remaining normals we compute the distance to the reference plane and take the maximum. Finally the mean value of all maxima obtained by varying the reference plane is computed. This will characterize the local properties of a candidate.

The shape of the response is evaluated by computing the best fitting ellipsoid given a cluster of sphere centers. The cluster has to be extracted from the Hough accumulator. For izolated polyps and haustral folds this is a straightforward job. Problems appear for polyps situated on haustral folds. A typical response for such a case is shown in Figure 4. It is observable that we have a small spherical structure corresponding to the polyp and the extended structure resembling the fold.

To be able to extract polyps correctly even in this case we start from a maxima, given by the non-maximum suppression algorithm and apply a distance weighted region growing technique. This technique takes at each step the neighbor with the highest value in the accumulator, weighted with the squared distance between the neighbor and the center of the cluster. Additionally a greedy region-growing algorithm, which at each step takes the neighbor with the highest value from the cluster is used. The two techniques give similar results for polyps and folds but give opposite results for a polyp on a haustral fold (see Figure 4), in this case the first method extracts only the polyp, while the second one extracts the main shape of the cluster.

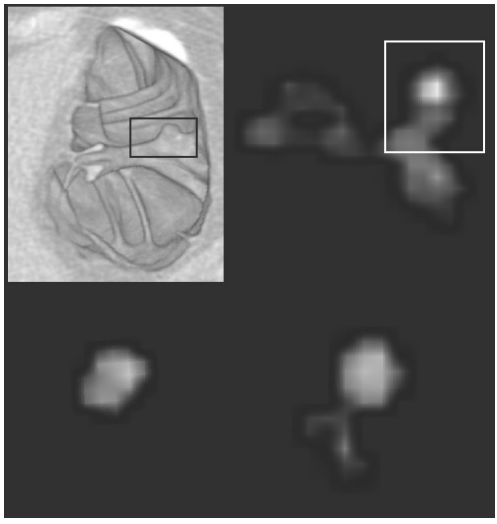

Figure 4: Initial polyp situated on a haustral fold (top left), the generated sphere centers (top right). On the bottom row the difference between the two region-growing algorithms is observable, while the weighted algorithm (left) extracts only the polyp, the greedy one (right) extracts the main shape of the region (polyp + haustra). Zooming factors are indicated by the two rectangles.

Once a cluster is extracted an ellipsoid is fitted to evaluate its shape. Generally the equation of the ellipsoid is:

$$\frac{(x-x_0)^2}{a^2} + \frac{(y-y_0)^2}{b^2} + \frac{(z-z_0)^2}{c^2} = 1$$

To reduce the number of parameters it is prefer-

able to translate the ellipsoid into the origin of the coordinate system and align it with the axis of the coordinate system, since we are only interested in the main axis of the ellipsoid. Lets assume a cluster $C = (P, V)$, with $P$ a set of $(x_i, y_i, z_i)$ tuples representing positions in the Hough accumulator and $V$ a set of values $(v_i)$, with $v_i$ being the value in the accumulator at $(x_i, y_i, z_i)$. The cluster is translated and centered around the origin, with factors given by $mean(P)$.

Eigen analysis is carried out and C is rotated using: $P^{'} = Eigen\_vector * P$, with $(P^{'}, V)$ the rotated cluster and $Eigen\_vector$ the eigen vector.

Finally we have to take into consideration that most of the cluster is inside the ellipsoid. That is why the $F_{el} = \frac{mean(V)}{v_i}$ term is introduced. Taking into account these assumptions the equation of the ellipsoid becomes:

$$\frac{x^2}{a^2} + \frac{y^2}{b^2} + \frac{z^2}{c^2} = F_{el}$$

This equation is solved for each cluster using a least square approximation technique. The matrix notation for the previous equation is:

$$\begin{bmatrix} & \dots & \\ x_i^2 & y_i^2 & z_i^2 \\ & \dots & \end{bmatrix} \cdot \begin{bmatrix} \frac{1}{a^2} \\ \frac{1}{b^2} \\ \frac{1}{c^2} \end{bmatrix} = \begin{bmatrix} \dots \\ \frac{mean(V)}{v_i} \\ \dots \end{bmatrix}$$

which can be seen as: $A.X = B$.

The values for $a$, $b$ and $c$ are given by:

$$X = (A^T.A)^{-1}.A^T.B$$

Finally all the above features are fed into the probabilistic classifier.

### 2.3 Classification

For the classification we used a probabilistic neural network (PNN), based on a radial basis architecture [10]. It consists of two layers, the first one computes the distance from the input vector to the training vectors. The second layer sums the contributions for each class of inputs to produce a vector of probabilities. Finally the maximum of these probabilities is chosen and the input is classified as belonging to that class.

The PNN is easy to train, a useful property since it will be trained after each new case, but it is somewhat slower when classifying since it has to compute distances to all the training samples. That is why we try to keep the training samples as low as possible, thus we select only the most representative samples for each case (samples for which the distance from the current samples is the highest). By this we want to obtain a training field containing representative examples for each class.

In our case only two classes were defined, polyps and false positive findings. Thus, the false positives were not divided into their representative classes like: haustral folds, colonic wall, insuflation tube and valve of Boyen. Also due to the low number of examples no difference was made between the different classes of polyps.

The output of the classier is considered as the final result of our CAD scheme and the results are presented to the reading radiologist.

## 3 Results

Twenty-six patients, 13 normal and 13 with 42 polyps of various sizes (Table 1) underwent CT colonography prior to conventional colonoscopy. Informed consent was obtained from all patients. The patient preparation consisted in the oral administration of 3 to 5 liter of precolon, an in-house developed tagging agent. In some cases the use of polyethylene glycol electrolyte solution was preferred. Immediately before CT colonography a bowel relaxant was injected intravenously. CO2 was insufflated using a bag system.

Table 1: Polyp distribution and detection results. (No = total number of polyps, TP = true positives)

| Type | No | Submerged | TP | Sensitivity |
|---|---|---|---|---|
| Flat | 4 | 1 | 1 | 33.33% |
| $< 5$ mm | 8 | 2 | 1 | 16.67% |
| 6-9 mm | 12 | 3 | 8 | 88.89% |
| $> 9$ mm | 14 | 1 | 12 | 92.30% |
| Tumor | 4 | 0 | 4 | 100% |
| Total | 42 | 7 | 26 | 74.29% |

CT colonography was performed on a multidetector CT (Multi Slice Helical CT; Volume Zoom, Siemens, Erlangen, Germany) using 4x1 mm detector configuration, 7 mm table feed per 0.5 s tube rotation, 0.8 mm reconstruction increment as well as 60 effective mAs and 120 keV. Patients

were scanned in both supine and prone positions, in breadth holds of 20 to 30 seconds. This resulted in 52 data-sets which were considered as input for our CAD system. On average the size of the acquired data sets was 247.07 MB. The image processing was done on an Intel Pentium III system running at 533 MHz and having 512 MB of RAM.

As a first step seed points were defined manually and then the whole CAD process was completed automatically. The mean segmentation threshold was 582 (CT number) and had a standard deviation of 31 units. The typical shape of the cumulative Laplacian histogram for abdominal images is shown in Figure 5.

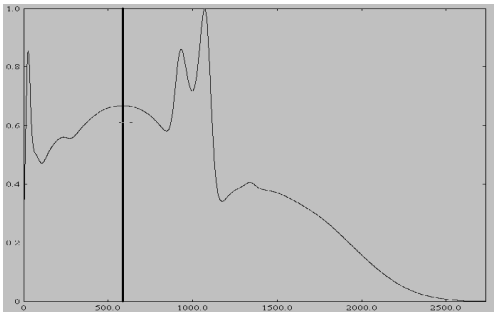


Figure 5: The cumulated Laplacian histogram for an abdominal image. The vertical line indicates the value of the extraction threshold.

Using conventional colonoscopy as standard of reference true positive (TP) and false positive (FP) findings were determined for each patient. The total number of polyps was 42, from these 7 were submerged under residual fluid and were not considered as false negative cases, since our method was not designed to detect them. The detection rate differentiated on polyp size is presented in Table 1. The average computation time for the whole CAD process as well as for different steps is shown in Table 2.

The total number of false positives was 127, which gives us a mean value of 2.82 false positive findings per data-set. The main causes for false positives are presented in Table 3.

## 4 Discussion and conclusion

Previously we considered the size of significant polyps as 10mm, but it became obvious that for screening purposes the size of detectable polyps had to be lowered. By establishing a lower value the advantages are twofold, on one hand polyps are detected and removed at an early stage, while on the other hand the screening interval can be increased.

Table 2: Average computation times, expressed in minutes.

| | |
|---|---|
| Segmentation | 1:47 |
| Normal incidence | 14:56 |
| Sphere fitting | 4:29 |
| Feature extraction | 0:16 |
| Neural analysis | 0:12 |
| Overall | 21:40 |

Table 3: False positives causes.

| Cause | Procent |
|---|---|
| Colonic wall | 33.86 % |
| Stool or fluid | 31.50 % |
| Haustral fold | 20.47 % |
| Ileocecal valve | 8.66 % |
| Insuflation tube | 5.51 % |

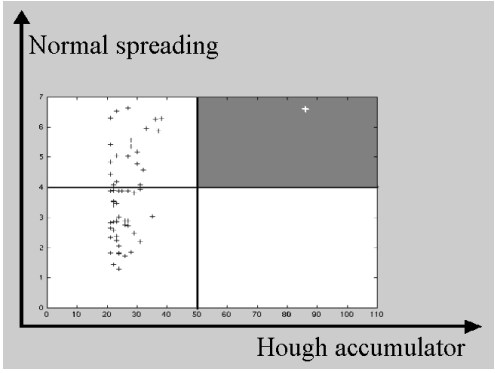


Figure 6: Polyp extraction based on simple thresholding. Only candidates in the dark region are selected.

The previous approach generated candidates using a simple thresholding operation on two features (value in the Hough accumulator and the normal distribution), see Figure 6. This was enough to detect large polyps but failed in other cases, in fact

smaller polyps could be detected at the cost of a large number of false positive findings. To limit the number of false positives high threshold values had to be established and thus smaller polyps were missed. That is why the feature set was extended and the classification method adapted accordingly.

By combining the surface normal and sphere fitting methods we tried to extract and use the advantages of both methods. In fact using the sphere fitting as an additional step we are able to make a better differentiation between polyps and haustral folds. Also using a Hough transform based method for sphere fitting the complexity of the classification problem is reduced.

Our previous method suffered from low sensitivity and also low specificity when trying to detect smaller polyps, that is why a better classification step was added. This is able to extract, based solely on implicit polyp properties, small polyps as well. The main advantage of PNN network is that it is easy to train and if the number of training samples is kept low than it has quick classification times as well.

Our results are comparable to those obtained by other authors [6], [7]. They show that there is a strong correlation between the size of the polyps and the number of false positives generated. Also it is obvious that for the time being this results (due to their low specificity) have to be inspected by a qualified radiologist. But using simple visualization methods like axial slices or volume rendered images he can quickly go through the list of candidates and discriminate between real and false positive findings.

Further improvements to our method are possible. First, a preprocessing step of eliminating the residual stool and fluid is needed, because these residues generate a large number of false positive findings and also 16.67% of polyps are submerged and can not be detected by the current technique. It has to be mentioned that further improvements can be done when selecting the training data set in order to end up with the most representative samples.

A fully automatic CAD technique is desired when thinking of applying the method for screening purposes. To achieve that a fully automatic segmentation method is needed.

We have presented a CAD technique that was evaluated on a significantly large number of CTC cases. Our algorithm showed high sensitivity results for polyps of 6mm or larger and a low number of 2.82 false positive findings per data set. These results show that our method is feasible, and it is useful for clinical studies. We can conclude that CAD will probably become the most common way of doing CTC, improving on current accuracy, efficiency and costs.

## 5 Acknowledgement

This work is part of the GOA/99/05 project: "Variability in Human Shape and Speech", financed by the Research Fund, K.U. Leuven, BELGIUM.

## References

[1] J.D. Potter et al., "Colon cancer: a review of the epidemiology", *Epidemol Rev 1993*, 15:pp. 449-545, 1993

[2] "Colorectal cancer - Oncology Channel", *http://www.oncologychannel.com/coloncancer/*

[3] D.J. Vining et al., "Virtual colonoscopy", *Radiology*, pp:193:446 (abstract), 1994

[4] Wolfgang Luboldt, Joel G. Fletcher, Thomas J. Vogl, "Colonography: current status, research directions and challenges. Update 2002", *Eur Radiol*, 12:pp 525-530, 2002

[5] G. Kiss et al., "Computer aided diagnosis for virtual colonography", *Proceedings 4th international conference on medical image computing and computer-assisted intervention - MICCAI2001, lecture notes in computer science*, 2208:pp 621-628, 2001

[6] S.B. Gokturk et al., "A Statistical 3-D Patter Processing Method for Computer-Aided Detection of Polyps in CT Colonography", *IEEE Transactions on Medical Imaging*, 20:pp 1251-1260, 2001

[7] H. Yoshida, J. Nappi., "3-D Computer-Aided Diagnosis Scheme for Detection of Colonic Polyps", *IEEE Transactions on Medical Imaging*, 20:pp 1261-1274, 2001

[8] D.M. Ballard, C.M. Brown, "Computer Vision", *Prentice Hall*, pp. 123-166, 1982

[9] R. Wiemker, V. Pekar, "Fast Computation of Isosurface Contour Spectra for Volume Visualization", *Proceedings Computer Assisted Radiology and Surgery CARS 2001*, 2001

[10] "Neural Network Toolbox User's guide", *www.mathworks.com*, 1992-2001